



Research article

Linearization and computation for large-strain visco-elasticity

Patrick Dondl¹, Martin Jesenko², Martin Kružík^{3,4,*} and Jan Valdman^{3,5}

¹ Department for Applied Mathematics, University of Freiburg, Germany

² University of Ljubljana, Faculty of Civil and Geodetic Engineering, Ljubljana, Slovenia

³ Institute of Information Theory and Automation, Czech Academy of Sciences, Praha 8, Czechia

⁴ Faculty of Civil Engineering, Czech Technical University, Thákurova 7, CZ-166 29 Praha 6, Czechia

⁵ Department of Mathematics, Faculty of Science, University of South Bohemia, České Budějovice, Czechia

* **Correspondence:** Email: kruzik@utia.cas.cz; Tel: +420266052395; Fax: +420286581419.

Abstract: Time-discrete numerical minimization schemes for simple visco-elastic materials in the Kelvin-Voigt rheology at high strains are not well posed because of the non-quasi-convexity of the dissipation functional. A possible solution is to resort to non-simple material models with higher-order gradients of deformations. However, this makes numerical computations much more involved. Here, we propose another approach that relies on local minimizers of the simple material model. Computational tests are provided that show a very good agreement between our model and the original.

Keywords: Kelvin-Voigt rheology; visco-elasticity; numerical scheme

1. Introduction

In-time-semidiscretized problems of nonlinear visco-elasticity in Kelvin-Voigt rheology lead to a sequence of minimization problems where a current solution depends on the previous one. More precisely, starting from an initial condition y^0 we must find for $k = 1, \dots, T/\tau$

$$y^k \in \operatorname{argmin}_y \int_{\Omega} \left(W(\nabla y) + \frac{1}{2\tau} D^2(\nabla y, \nabla y^{k-1}) \right) dx, \quad (1.1)$$

where $\tau > 0$ is a time step, T is a final time, W is an elastic energy density and D is a dissipation due to viscosity. However, physically acceptable dissipation functions are not (Morrey) quasiconvex [1]. As we are interested in the limit for $\tau \rightarrow 0$, the problem (1.1) does not necessarily have a minimizer

since, for small τ , the non-quasiconvexity of D cannot be compensated for by any convexity of W . This suggests microstructure formation due to rapidly oscillating deformation gradients, which, however, is not observed in reality. The aim of this work is to explore this discrepancy.

Due to dissipative effects, we expect y^k to be found in a small neighborhood of y^{k-1} . Thus, the minimization in (1.1) should be local. For that reason, we linearize the energy functional in (1.1) in the spirit of [7]. Thus, we obtain a quadratic energy contribution that stems from the dissipation and stress of the elastic energy. The resulting functional is not coercive, but, in spite of this, minimizers exist, as we show.

We perform numerical experiments by comparing the original nonlinear scheme in (1.1) with our linearized scheme for small time steps that show very good quantitative agreement. Moreover, both schemes satisfy an energy balance.

2. Modeling of nonlinear visco-elasticity

If we neglect inertial effects, the deformation $y : [0, T] \times \Omega \rightarrow \mathbb{R}^d$ of a nonlinear viscoelastic material in Kelvin-Voigt rheology obeys the following system of equations

$$-\operatorname{div}(\partial_F W(\nabla y) + \partial_{\dot{F}} R(\nabla y, \nabla \dot{y})) = f \text{ in } [0, T] \times \Omega, \quad (2.1a)$$

$$(\partial_F W(\nabla y) + \partial_{\dot{F}} R(\nabla y, \nabla \dot{y}))n = g \text{ on } [0, T] \times \Gamma_N, \quad (2.1b)$$

$$y = y_D \text{ on } [0, T] \times \Gamma_D, \quad (2.1c)$$

$$y(0, \cdot) = y^0 \text{ in } \Omega, \quad (2.1d)$$

Here, $[0, T]$ is a process time interval, $\Omega \subset \mathbb{R}^d$ ($d = 2$ or $d = 3$) is a smooth bounded domain representing the reference configuration, $\Gamma_D \cup \Gamma_N$ is a disjoint partition of $\partial\Omega$ such that Γ_D has a positive $(d - 1)$ -dimensional Hausdorff measure. In addition, $f : [0, T] \times \Omega \rightarrow \mathbb{R}^d$ is a density of body forces and $g : [0, T] \times \Gamma_N \rightarrow \mathbb{R}^d$ is a density of surface forces. We also impose boundary data $y_D : [0, T] \times \Gamma_D \rightarrow \mathbb{R}^d$ and an initial condition $y^0 : \Omega \rightarrow \mathbb{R}^d$.

The properties of the material are described by the stored energy density $W : \mathbb{R}^{d \times d} \rightarrow [0, \infty]$, where its gradient represents the first Piola-Kirchhoff stress tensor, and by a (pseudo)potential of dissipative forces $R : \mathbb{R}^{d \times d} \times \mathbb{R}^{d \times d} \rightarrow [0, \infty)$.

The stress tensor $S(F, \dot{F}) := \partial_{\dot{F}} R(F, \dot{F})$ has its origin in the viscous dissipative mechanisms of the material. Naturally, we require $R(F, \dot{F}) \geq R(F, 0) = 0$. The viscous stress tensor must comply with the time-continuous frame-indifference principle, meaning that for all $F, \dot{F} \in \mathbb{R}^{d \times d}$

$$S(F, \dot{F}) = F \tilde{S}(C, \dot{C})$$

with some $\tilde{S} : \mathbb{R}_{\text{sym}}^{d \times d} \times \mathbb{R}_{\text{sym}}^{d \times d} \rightarrow \mathbb{R}_{\text{sym}}^{d \times d}$ where $C = F^\top F$ and $\dot{C} = \dot{F}^\top F + F^\top \dot{F}$. This condition constrains R so that (see [1, 2, 12])

$$R(F, \dot{F}) = \tilde{R}(C, \dot{C}) \quad (2.2)$$

for some non-negative function \tilde{R} such that $\tilde{R}(C, 0) = 0$. In other words, R must depend on the right Cauchy-Green strain tensor C and its time derivative \dot{C} . On the other hand, this property makes the analysis of (2.1) very difficult. To our knowledge, the existence of a solution has not been established

so far. If the stored energy is enriched by the second gradient of deformation, the existence results are available in various settings; see [8, 11] in three dimensions and [3, 12] in one dimension.

In any case, a standard approach to obtain solutions for such evolution problems is to introduce an implicit time discretization. For simplicity, we will assume that y_D is constant in time in the sequel. Let $\tau > 0$ be a time step such that $T/\tau \in \mathbb{N}$. Given an initial condition y_τ^0 , for $k = 1, \dots, T/\tau$, we now want to find y_τ^k such that

$$\begin{aligned} -\operatorname{div}\left(\partial_F W(\nabla y_\tau^k) + \partial_{\dot{F}} R(\nabla y_\tau^k, \nabla \frac{y_\tau^k - y_\tau^{k-1}}{\tau})\right) &= f_\tau^k := \tau^{-1} \int_{(k-1)\tau}^{k\tau} f(s, \cdot) \, ds \quad \text{in } \Omega, \\ \left(\partial_F W(\nabla y_\tau^k) + \partial_{\dot{F}} R(\nabla y_\tau^k, \nabla \frac{y_\tau^k - y_\tau^{k-1}}{\tau})\right)n &= g_\tau^k := \tau^{-1} \int_{(k-1)\tau}^{k\tau} g(s, \cdot) \, ds \quad \text{on } \Gamma_N, \\ y_\tau^k &= y_D \quad \text{on } \Gamma_D, \end{aligned} \quad (2.3)$$

that is, y_τ^k should solve a discretized version of (2.1). In the following, we summarize our setting and the basic assumptions used to treat this incremental time minimization problem.

Stored elastic energy and body forces: We assume that the stored elastic energy $W : \mathbb{R}^{d \times d} \rightarrow [0, \infty]$ has the following properties:

- (i) W is smooth on matrices with positive determinants,
- (ii) $W(QF) = W(F)$ for all $F \in \mathbb{R}^{d \times d}$ and all proper rotations $Q \in \operatorname{SO}(d)$,
- (iii) $W(F) \geq c(-1 + |F|^p)$ for all $F \in \mathbb{R}^{d \times d}$, and for some $c > 0$, $p > 1$,
- (iv) $W(F) = +\infty$ if $\det F \leq 0$, and $\lim_{\det F \rightarrow 0} W(F) = +\infty$.

We introduce the nonlinear elastic energy $\phi_\tau^k : W^{1,p}(\Omega; \mathbb{R}^d) \rightarrow [0, \infty]$ by

$$\phi_\tau^k(y) = \int_\Omega W(\nabla y(x)) \, dx - \int_\Omega f_\tau^k(x) \cdot y(x) \, dx - \int_{\Gamma_N} g_\tau^k(x) \cdot y(x) \, dS \quad (2.5)$$

for $y : W^{1,p}(\Omega; \mathbb{R}^d) \rightarrow \mathbb{R}^d$. In what follows, we assume that $\phi_\tau^k : W^{1,p}(\Omega; \mathbb{R}^d) \rightarrow \mathbb{R} \cup \{+\infty\}$ is sequentially weakly lower semicontinuous.

Dissipation potential and viscous stress: Consider a time-dependent deformation $y : [0, T] \times \Omega \rightarrow \mathbb{R}^d$. Viscosity is not only related to strain $\nabla y(t, x)$, but also to strain rate $\nabla \dot{y}(t, x)$ and can be expressed in terms of dissipation potential $R(\nabla y, \nabla \dot{y})$. An admissible potential has to satisfy the frame indifference in the sense (see [1, 12])

$$R(F, \dot{F}) = R(QF, Q(\dot{F} + AF)) \quad \forall Q \in \operatorname{SO}(d), A \in \operatorname{Skew}(d) \quad (2.6)$$

for all $F \in \operatorname{GL}_+(d)$ and $\dot{F} \in \mathbb{R}^{d \times d}$, where

$$\operatorname{GL}_+(d) = \{F \in \mathbb{R}^{d \times d} : \det F > 0\}, \quad \operatorname{Skew}(d) = \{A \in \mathbb{R}^{d \times d} : A = -A^\top\}.$$

Following the discussion in [12, Section 2.2], from the point of view of modeling, it is much more convenient to postulate the existence of a (smooth) global distance $D : \operatorname{GL}_+(d) \times \operatorname{GL}_+(d) \rightarrow [0, \infty)$ that

satisfies $D(F, F) = 0$ for all $F \in \text{GL}_+(d)$. From this distance, an associated dissipation potential R can be calculated by

$$R(F, \dot{F}) := \lim_{\varepsilon \rightarrow 0} \frac{1}{2\varepsilon^2} D^2(F + \varepsilon \dot{F}, F) = \frac{1}{4} \partial_{F_1}^2 D^2(F, F)[\dot{F}, \dot{F}] \quad (2.7)$$

for $F \in \text{GL}_+(d)$, $\dot{F} \in \mathbb{R}^{d \times d}$. Above, the fourth-order tensor $\partial_{F_1}^2 D^2(F_1, F_2)$ denotes the Hessian of D^2 in the direction of F_1 at (F_1, F_2) .

For the sake of simplicity, in the present work we use

$$D(F_1, F_2) = |C_1 - C_2|,$$

where $C_i = F_i^\top F_i$ for $i = 1, 2$ and $|A|^2 = \text{tr}(A^\top A)$. In this case, a direct computation yields

$$R(F, \dot{F}) = 2|\text{sym}(F^\top \dot{F})|^2. \quad (2.8)$$

For justification of this choice for D and for further examples of admissible dissipation distances, we refer the reader to [12, Section 2.3].

Now, the solutions to (2.3) can *formally* be written as solutions of the following sequence of problems:

$$\begin{aligned} &\text{For a given } y_\tau^{k-1} \in W^{1,p}(\Omega; \mathbb{R}^d) \text{ with } y_\tau^{k-1} = y_D \text{ on } \Gamma_D \\ &\text{minimize } \phi_\tau^k(y) + \frac{1}{2\tau} \int_\Omega D^2(\nabla y, \nabla y_\tau^{k-1}) \, dx \\ &\text{subject to } y \in W^{1,p}(\Omega; \mathbb{R}^d), y = y_D \text{ on } \Gamma_D. \end{aligned} \quad (2.9)$$

The non-quasiconvexity of $F \mapsto D(F, G)$ for a given G , see [6], would suggest that an energy-minimizing microstructure is formed in the viscous relaxation of materials. However, such a microstructure has not been observed in experiments. Thus, we propose that, in such a viscous evolution, the energy landscape is only explored in a small neighborhood of the current state, instead of the global minimization suggested by (2.9). Therefore, our approach is to minimize in each time step a problem that is linearized around y_τ^{k-1} in a suitable sense.

3. Linear visco-elasticity

To motivate our linearization approach for this implicit time-discretization problem, we first consider the case of (already) linearized visco-elasticity. Here, we simply recover the original evolution equations, which (neglecting any forces) are given by the linear Kelvin-Voigt visco-elasticity problem

$$\begin{aligned} -\text{div}(\mathbb{C}\nabla u + \mathbb{D}\nabla \dot{u}) &= 0 && \text{in } [0, T] \times \Omega, \\ u &= u_D && \text{on } \Gamma_D, \\ u(0, \cdot) &= u^0 && \text{in } \Omega. \end{aligned} \quad (3.1)$$

Here \mathbb{C} and \mathbb{D} are positive definite fourth-order tensors of elasticity and viscosity coefficients, respectively. Note that in this linearized setting, we work with a displacement field u instead of the deformation y .

The variational formulation for the linear counterpart of (2.3) reads: For a given $u_\tau^{k-1} \in W^{1,2}(\Omega; \mathbb{R}^d)$ with $u_\tau^{k-1} = u_D$ on Γ_D , find the minimizer u_τ^k of

$$u \mapsto \frac{1}{2} \int_{\Omega} \mathbb{C} \nabla u : \nabla u \, dx + \frac{1}{2\tau} \int_{\Omega} \mathbb{D}(\nabla u - \nabla u_\tau^{k-1}) : (\nabla u - \nabla u_\tau^{k-1}) \, dx. \quad (3.2)$$

under the constraints $u \in W^{1,2}(\Omega; \mathbb{R}^d)$ and $u = u_D$ on Γ_D . Since the functional is quadratic and convex in ∇u , the minimizer exists in fact and is unique. It is clear that this iterative minimization scheme, in the limit of small time steps τ , leads to a solution of (3.1).

Our idea is to reformulate the minimization problem to (3.2) in terms of minimizing an increase in displacement. More precisely, we write $u = u_\tau^{k-1} + \tau z$ and minimize

$$z \mapsto \frac{1}{2} \int_{\Omega} \left(\mathbb{C} \nabla u_\tau^{k-1} : \nabla u_\tau^{k-1} + 2\tau \mathbb{C} \nabla u_\tau^{k-1} : \nabla z + \tau^2 \mathbb{C} \nabla z : \nabla z + \tau \mathbb{D} \nabla z : \nabla z \right) \, dx, \quad (3.3)$$

or, equivalently, after subtracting the constant first term and rescaling by $\frac{1}{\tau}$, minimize

$$z \mapsto \frac{1}{2} \int_{\Omega} \left(2\mathbb{C} \nabla u_\tau^{k-1} : \nabla z + \tau \mathbb{C} \nabla z : \nabla z + \mathbb{D} \nabla z : \nabla z \right) \, dx \quad (3.4)$$

under the constraints $z \in W^{1,2}(\Omega; \mathbb{R}^d)$ and $z = 0$ on Γ_D . We observe that the second term is dominated by the third for small τ . Therefore, we minimize

$$z \mapsto \frac{1}{2} \int_{\Omega} \left(2\mathbb{C} \nabla u_\tau^{k-1} : \nabla z + \mathbb{D} \nabla z : \nabla z \right) \, dx \quad (3.5)$$

instead. This problem admits a unique minimizer z that solves the associated Euler-Lagrange equation

$$-\operatorname{div}(\mathbb{C} \nabla u_\tau^{k-1} + \mathbb{D} \nabla z) = 0. \quad (3.6)$$

Then $u_\tau^k = u_\tau^{k-1} + \tau z$ fulfills

$$-\operatorname{div}(\mathbb{C} \nabla u_\tau^{k-1} + \frac{1}{\tau} \mathbb{D} \nabla (u_\tau^k - u_\tau^{k-1})) = 0. \quad (3.7)$$

We note that this is an explicit Euler time step for the original evolution equation (3.1), where the standard minimization of movement results in the implicit scheme

$$-\operatorname{div}(\mathbb{C} \nabla u_\tau^k + \frac{1}{\tau} \mathbb{D} \nabla (u_\tau^k - u_\tau^{k-1})) = 0. \quad (3.8)$$

Note that we obtained this solution from the linearized functional (3.5) and not from (3.4). This suggests that we can write a minimization problem in the velocity z for the dissipated power and still obtain a reasonable time-stepping scheme for linearized Kelvin-Voigt visco-elasticity.

Emboldened by this result for the linearized problem, for which existence of solutions is of course already well known, we attempt to treat the fully non-linear case.

4. The limit for the nonlinear visco-elastic minimization problem

We now consider again the fully nonlinear implicit time-stepping problem for visco-elasticity.

4.1. Linearization of the minimization problem

Neglecting forces, we start with the (ill-posed) time-step problem of finding y_τ^k minimizing the problem

$$y \mapsto \int_{\Omega} \left(W(\nabla y) + \frac{1}{2\tau} D^2(\nabla y, \nabla y_\tau^{k-1}) \right) dx. \quad (4.1)$$

This minimization problem can be restricted to include appropriate boundary conditions. Let us, as in the linear case, see (3.3), rewrite this problem in terms of minimizing increments. By substituting $y_\tau^k = y_\tau^{k-1} + \tau z_\tau^k$, we arrive at the problem of finding z_τ^k as a minimizer of

$$z \mapsto \int_{\Omega} \left(W(\nabla y_\tau^{k-1} + \tau \nabla z) + \frac{1}{2\tau} D^2(\nabla y_\tau^{k-1} + \tau \nabla z, \nabla y_\tau^{k-1}) \right) dx. \quad (4.2)$$

We notice that for small τ the terms that are linear in τ play the crucial role in the minimization. Therefore, let us for a suitable $y : \Omega \rightarrow \mathbb{R}^d$ and any $\tau > 0$ define a singularly perturbed functional

$$\mathcal{F}_{y,\tau}(z) := \frac{1}{\tau} \int_{\Omega} \left(W(\nabla y + \tau \nabla z) - W(\nabla y) + \frac{1}{2\tau} D^2(\nabla y + \tau \nabla z, \nabla y) \right) dx. \quad (4.3)$$

Notice that the functionals in (4.2) and $\mathcal{F}_{y_\tau^{k-1},\tau}$ of (4.3) are equivalent with respect to minimization. Since τ is small, let us explore the limit $\lim_{\tau \rightarrow 0} \mathcal{F}_{y,\tau}$ for a fixed y . We begin with some pointwise assessments of the density of the functional (4.3). Therefore, for simplicity, we write $Y := \nabla y$ and $Z := \nabla z$ and assume $\det Y \geq c > 0$ and $|Y|, |Z| \leq M < \infty$.

Since W is smooth, it holds

$$W(Y + \tau Z) = W(Y) + \partial_F W(Y) : \tau Z + \frac{1}{2} \partial_{F^2}^2 W(Y + \xi Z) \tau Z : \tau Z$$

for some $\xi \in [0, \tau]$. Thus, the first two terms in (4.3) can be rewritten as

$$\frac{W(Y + \tau Z) - W(Y)}{\tau} = \partial_F W(Y) : Z + \frac{\tau}{2} \partial_{F^2}^2 W(Y + \xi Z) Z : Z. \quad (4.4)$$

For the third term, we have (considering $D(F, G) = |F^\top F - G^\top G|$)

$$\begin{aligned} \frac{1}{2\tau^2} D(Y + \tau Z, Y)^2 &= \frac{1}{2\tau^2} |(Y + \tau Z)^\top (Y + \tau Z) - Y^\top Y|^2 \\ &= \frac{1}{2} |Z^\top Y + Y^\top Z + \tau Z^\top Z|^2 \\ &= \frac{1}{2} |Z^\top Y + Y^\top Z|^2 + \tau (Z^\top Y + Y^\top Z) : (Z^\top Z) + \frac{\tau^2}{2} |Z^\top Z|^2 \\ &= 2 |\text{sym}(Y^\top Z)|^2 + 2\tau Y : ZZ^\top Z + \frac{\tau^2}{2} |Z^\top Z|^2 \end{aligned}$$

We note that terms containing τ become negligible since we have a uniform upper bound on admissible $|Y|$ and $|Z|$. Then

$$\frac{W(Y + \tau Z) - W(Y)}{\tau} + \frac{1}{2\tau^2} D(Y + \tau Z, Y)^2 = \partial_F W(Y) : Z + 2 |\text{sym}(Y^\top Z)|^2 + R(\tau, Y, Z) \quad (4.5)$$

with the remainder satisfying

$$|\mathcal{R}(\tau, Y, Z)| \leq C\tau|Z|^2 + 2\tau|Y||Z|^3 + \frac{\tau^2}{2}|Z|^4 \quad (4.6)$$

for some $C = C_{c,M} > 0$. Therefore, if $y, z \in W^{1,\infty}(\Omega; \mathbb{R}^d)$ and $\det \nabla y \geq c > 0$, we obtain the pointwise convergence

$$\lim_{\tau \rightarrow 0} \mathcal{F}_{y,\tau}(z) = \int_{\Omega} \left(\partial_F W(\nabla y) : \nabla z + 2|\text{sym}((\nabla y)^\top \nabla z)|^2 \right) dx.$$

This immediately leads to the following approximation result.

Lemma 4.1. *Let $y \in W^{1,\infty}(\Omega; \mathbb{R}^d)$ with $\det \nabla y \geq c > 0$. On the set $\{z \in W^{1,\infty}(\Omega; \mathbb{R}^d) : \|\nabla z\|_{L^\infty} \leq M\}$, the functional $\mathcal{F}_{y,\tau}$ defined in (4.3) can be uniformly approximated by*

$$\mathcal{F}_y(z) = \int_{\Omega} \left(\partial_F W(\nabla y) : \nabla z + 2|\text{sym}((\nabla y)^\top \nabla z)|^2 \right) dx \quad (4.7)$$

so that

$$|\mathcal{F}_{y,\tau}(z) - \mathcal{F}_y(z)| \leq \tau C$$

where C depends only on $\Omega, \|\nabla y\|_{L^\infty}, c, M$, and W .

Hence, the solution to the visco-elastic evolution problem should be well approximated by

$$y^k = y^{k-1} + \hat{\tau} z \quad (4.8)$$

for small $\hat{\tau}$, with z calculated as the minimizer of (4.7) (with $y = y^{k-1}$) in each time step. The heuristic interpretation of this method is that we derived a linearized functional (depending on given state) whose minimizer is the velocity in the evolution problem corresponding to the state. Equation (4.8) then is nothing but a forward Euler time step with this velocity.

4.2. Existence of minimizers

Let us explore the properties of the functional in (4.7). In the following, restricting ourselves to the physically relevant case $d = 3$, we fix $y \in C^2(\bar{\Omega}; \mathbb{R}^3)$ so that $\inf_{x \in \Omega} \det \nabla y > 0$.

We immediately notice that the quadratic form in the energy (4.7) is not fully coercive, as $2|\text{sym}((\nabla y)^\top \nabla z)|^2 = 0$ for any skew-symmetric $(\nabla y)^\top \nabla z$. This is in a sense similar to the problem of linearized elasticity. It appears that the presence of the first term $\partial_F W(\nabla y) : \nabla z$ means that \mathcal{F}_y is not bounded from below for directions ∇z where linearized dissipation vanishes. However, this is not the case since the second Piola-Kirchhoff stress tensor $(\nabla y)^{-1} \partial_F W(\nabla y)$ is always symmetric.

For the sake of clarity, let us denote the energy density by

$$f_Y(Z) = \partial_F W(Y) : Z + 2|\text{sym}(Y^\top Z)|^2. \quad (4.9)$$

If $Y^{-1} \partial_F W(Y)$ is symmetric, for any $Z \in \mathbb{R}^{3 \times 3}$ it holds

$$\partial_F W(Y) : Z = Y Y^{-1} \partial_F W(Y) : Z = Y^{-1} \partial_F W(Y) : Y^\top Z = Y^{-1} \partial_F W(Y) : \text{sym}(Y^\top Z). \quad (4.10)$$

Therefore,

$$\begin{aligned} f_Y(Z) &= \partial_F W(Y) : Z + 2|\text{sym}(Y^\top Z)|^2 \\ &= Y^{-1} \partial_F W(Y) : \text{sym}(Y^\top Z) + 2|\text{sym}(Y^\top Z)|^2 \\ &= 2|\frac{1}{4}Y^{-1} \partial_F W(Y) + \text{sym}(Y^\top Z)|^2 - \frac{1}{8}|Y^{-1} \partial_F W(Y)|^2. \end{aligned}$$

Therefore, the minimum of f_Y is $-\frac{1}{8}|Y^{-1} \partial_F W(Y)|^2$ and is achieved at Z for which it holds that $\text{sym}(Y^\top Z) = -\frac{1}{4}Y^{-1} \partial_F W(Y)$, i.e., the set of minimizers is $-\frac{1}{4}(YY^\top)^{-1} \partial_F W(Y) + Y^{-\top} \text{Skew}(3)$. Moreover, we have

$$f_Y(Z) \geq 2|\text{sym}(Y^\top Z)|^2 - |Y^{-1} \partial_F W(Y)| \cdot |\text{sym}(Y^\top Z)|$$

Therefore, the density f_Y and, consequently, the functional \mathcal{F}_y are bounded from below.

Now we consider the lack of coercivity since the functional depends only on $\text{sym}((\nabla y)^\top \nabla z)$. Here, we rely mainly on the results in [13]. Let us start by determining the subspace

$$\mathcal{N}_y = \{z \in W^{1,2}(\Omega; \mathbb{R}^3) : \text{sym}((\nabla y)^\top \nabla z) = 0\}.$$

First, we notice

$$\text{sym}((\nabla y)^\top \nabla z) = 0 \iff \text{sym}(\nabla z (\nabla y)^{-1}) = 0.$$

From Lemma 4.1 in [13] follows a higher regularity, namely $z \in C^2(\overline{\Omega}; \mathbb{R}^3)$ and $\nabla z (\nabla y)^{-1} \in C^{1,1/2}(\overline{\Omega}; \mathbb{R}^{3 \times 3})$. In Corollary 3.10 in [13] it was shown that if we have matrix fields $A, B \in C^1(\overline{\Omega}; \mathbb{R}^{3 \times 3})$ such that A is skew-symmetric and $B = \nabla \psi$, then

$$\text{curl}(AB) = 0 \implies A \text{ is constant.}$$

For $z \in \mathcal{N}_y$, the matrix field $A = \nabla z (\nabla y)^{-1}$ is skew-symmetric. If we take $B = \nabla y$, all assumptions are fulfilled, since

$$\text{curl}(AB) = \text{curl}(\nabla z (\nabla y)^{-1} \nabla y) = \text{curl} \nabla z = 0.$$

Therefore, A is constant and therefore $\nabla z = A \nabla y$. Consequently, $z = a + Ay$ for some vector $a \in \mathbb{R}^3$. Equivalently, $z = a + \omega \times y$ for some vectors $a, \omega \in \mathbb{R}^3$. Thus, we have shown

$$\mathcal{N}_y = \{z \in W^{1,2}(\Omega; \mathbb{R}^3) : \text{sym}((\nabla y)^\top \nabla z) = 0\} = \mathbb{R}^3 + \text{Skew}(3)y.$$

It is a 6-dimensional subspace.

Theorem 4.2. For a given $y \in C^2(\overline{\Omega}; \mathbb{R}^3)$ with $\det \nabla y > 0$, let us consider the functional

$$\mathcal{F}_y(z) = \int_{\Omega} \left(\partial_F W(\nabla y) : \nabla z + 2|\text{sym}((\nabla y)^\top \nabla z)|^2 \right) dx.$$

- (a) \mathcal{F}_y admits a unique minimizer on any subspace $H \subset W^{1,2}(\Omega; \mathbb{R}^3)$ with $H \cap \mathcal{N}_y = \{0\}$. This includes the case $H = \{z \in W^{1,2}(\Omega; \mathbb{R}^3) : z|_{\Gamma_D} = 0\}$ for some smooth $\Gamma_D \subset \partial\Omega$ with $\mathcal{H}^2(\Gamma_D) > 0$.
- (b) On the whole $W^{1,2}(\Omega; \mathbb{R}^3)$ minimizers exist and are unique up to an addition of elements from \mathcal{N}_y .

The proof will rely on generalized Korn's second inequality. For the proof, see Corollaries 4.6, 4.7, and Section 5 in [13].

Lemma 4.3 (Generalized Korn's second inequality). *Let $\Omega \subset \mathbb{R}^3$ be a Lipschitz domain, and $y \in C^1(\bar{\Omega}; \mathbb{R}^3)$ with $\det \nabla y > 0$. Then*

$$z \mapsto \|\operatorname{sym}((\nabla y)^\top \nabla z)\|_{L^2(\Omega)} + \|z\|_{L^2(\Omega)}$$

is a norm on $W^{1,2}(\Omega; \mathbb{R}^3)$ that is equivalent to $\|\cdot\|_{W^{1,2}(\Omega)}$.

Generalizing the standard Korn's inequality, one proves that for any subspace $H \subset W^{1,2}(\Omega; \mathbb{R}^3)$ with $H \cap \operatorname{Skew}(3)y = \{0\}$ there exists a constant C such that for every $z \in H$

$$\|\operatorname{sym}((\nabla y)^\top \nabla z)\|_{L^2(\Omega)} \geq C \|\nabla z\|_{L^2(\Omega)}.$$

Proof of Theorem 4.2. First, consider a subspace H with $H \cap \mathcal{N}_y = \{0\}$. The functional \mathcal{F}_y is strictly convex on H . This can be easily seen since, for a given $Y \in \mathbb{R}^{3 \times 3}$, the function is

$$f_Y(Z) = Y^{-1} \partial_F W(Y) : \operatorname{sym}(Y^\top Z) + 2|\operatorname{sym}(Y^\top Z)|^2$$

is a composition of a linear function $Z \mapsto \operatorname{sym}(Y^\top Z)$ and a strictly convex function $X \mapsto Y^{-1} \partial_F W(Y) : X + 2|X|^2$. Moreover, as

$$\mathcal{F}_y(z) \geq C \|\operatorname{sym}((\nabla y)^\top \nabla z)\|_{L^2(\Omega)} - C \geq C \|\nabla z\|_{L^2(\Omega)} - C,$$

there is a unique minimizer z_H on H . We refer to [13, Theorem 4.3] for the proof that (a) applies to $\{z \in W^{1,2}(\Omega) : z|_{\Gamma_D} = 0\}$, that is, $\{z \in W^{1,2}(\Omega) : z|_{\Gamma_D} = 0\} \cap \mathcal{N}_y = \{0\}$.

For the whole space case, let $H = \mathcal{N}_y^\perp$ be the orthogonal complement of \mathcal{N}_y in $W^{1,2}(\Omega; \mathbb{R}^3)$. By (a), there is a unique minimizer $z_{\mathcal{N}_y^\perp}$ on \mathcal{N}_y^\perp . Therefore, \mathcal{F}_y admits a minimizer in $W^{1,2}(\Omega; \mathbb{R}^3)$, and the set of all minimizers reads

$$z_{\mathcal{N}_y^\perp} + \mathcal{N}_y.$$

□

Remark 4.4. Since by (2.8)

$$\mathcal{F}_y(z) = \int_{\Omega} \left(\partial_F W(\nabla y) : \nabla z + R(\nabla y, \nabla z) \right) dx,$$

the Euler-Lagrange equation for the functional \mathcal{F}_y is

$$0 = -\operatorname{div} \left(\partial_F W(\nabla y) + \partial_F R(\nabla y, \nabla z) \right) \quad (4.11)$$

or

$$0 = -\operatorname{div} \left(\partial_F W(\nabla y) + 2\nabla y (\nabla z)^\top \nabla y + 2\nabla y (\nabla y)^\top \nabla z \right). \quad (4.12)$$

Let us return to (4.8) and suppose that z is a minimizer of $\mathcal{F}_{y^{k-1}}$. By plugging $z = (y^k - y^{k-1})/\tau$ in (4.12), we arrive at

$$-\operatorname{div} \left(\partial_F W(\nabla y^{k-1}) + \partial_F R(\nabla y^{k-1}, \frac{\nabla y^k - \nabla y^{k-1}}{\tau}) \right) = 0. \quad (4.13)$$

Since this is a simple time discretization of the original evolution equation (2.1a), we conjecture that our linearization method yields a solution of the original nonlinear visco-elastic problem. The convergence study below already suggests that the energy-dissipation equality is satisfied by our method.

5. Numerical results

We now consider a numerical implementation of the time-step method given in (4.8), where the velocity z is computed in each time step minimizing (4.7). For simplicity, we denote the time-step size here again by τ . Our implementation is based on finite elements, so we approximate

$$y^{k-1} \approx y_h^{k-1} = \sum_j (\mathbf{y}^{k-1})_j \phi_j$$

with a vector \mathbf{y}^{k-1} of degrees of freedom and finite element basis functions ϕ_j . In each time step we thus solve a linear system of the form

$$K\mathbf{z} = \mathbf{b},$$

where the symmetric system matrix is given by

$$K_{ij} = \int_{\Omega} c \left((\nabla \phi_i)^\top \nabla y_h^{k-1} + (\nabla y_h^{k-1})^\top \nabla \phi_i \right) : \left((\nabla \phi_j)^\top \nabla y_h^{k-1} + (\nabla y_h^{k-1})^\top \nabla \phi_j \right) dx \quad (5.1)$$

corresponding to the linearization of a nonlinear dissipation potential $D(F, G) = c|F^\top F - G^\top G|$. Compared to the previous discussion, we introduce a scaling parameter $c > 0$. The vector on the right-hand side is

$$\mathbf{b}_i = - \int_{\Omega} \left(\partial_F W(y_h^{k-1}) \right) : \nabla \phi_i dx.$$

The linear system is solved using the sparse direct Cholesky solver CHOLMOD [5] after a small shift of K (which, without boundary conditions, is only positive semidefinite) by δM (with finite element mass matrix M) to ensure positive definiteness. In all numerical experiments below, the value of δ has been fixed at $1 \cdot 10^{-8}$.

Finally we compute

$$\mathbf{y}^k = \mathbf{y}^{k-1} + \tau \mathbf{z} \quad (5.2)$$

and iterate this procedure. The finite element system can be endowed with appropriate boundary conditions, body forces, and surface tractions in the usual way. In the following we use the Neo-Hookean material model

$$W(F) = \frac{\mu}{2} (|F|^2 - 3 - 2 \log \det F) + \frac{\lambda}{2} (\det F - 1)^2 \quad (5.3)$$

with Lamé parameters μ and λ . All 3d simulations are performed using P2 finite elements on a tetrahedral mesh.

Experiment 1: a visco-elastic plate. In [8] a rigorous thin-plate limit for nonlinear visco-elastic materials was derived in the Föppl–von Kármán-scaling regime. Numerical experiments for thin-plate equations were performed in [9] combining Bogner-Fox-Schmit (BFS) finite elements [4, 14] for out-of-plane deformation $v: \omega \rightarrow \mathbb{R}$ and Q1 elements for in-plane deformation $u: \omega \rightarrow \mathbb{R}^2$ in the plate domain $\omega = (-1, 1)^2 \subset \mathbb{R}^2$. We use this setting as a first test case for our method, computing the visco-elastic relaxation of an initially deformed plate with clamped boundary conditions. As an initial condition, we choose

$$v(x_1, x_2) = (x_1 - 1)^2(x_2 - 1)^2, \quad u(x_1, x_2) = 0.$$

The thin-plate model minimizes the energy $\phi(u, v) + \frac{1}{2\tau} \mathcal{D}^2((u_{n-1}, v_{n-1}), (u, v))$, where the von Kármán energy functional ϕ is defined as

$$\phi(u, v) := \int_S \frac{1}{2} Q_W^2(e(u) + \frac{1}{2} \nabla v \otimes \nabla v) + \frac{1}{24} Q_W^2(\nabla^2 v) \, dx \quad (5.4)$$

and the global dissipation distance \mathcal{D} as

$$\begin{aligned} \mathcal{D}((u_0, v_0), (u_1, v_1)) := & \int_S \left(Q_D^2(e(u_1) - e(u_0) + \frac{1}{2} \nabla v_1 \otimes \nabla v_1 - \frac{1}{2} \nabla v_0 \otimes \nabla v_0) \right. \\ & \left. + \frac{1}{12} Q_D^2(\nabla^2 v_1 - \nabla^2 v_0) \right)^{1/2} \, dx \quad (5.5) \end{aligned}$$

respectively. As Q_W^2 and Q_D^2 we take the limiting Föppl–von Kármán plate material, i.e.,

$$Q_W^2(G) := \frac{2\mu\lambda}{2\mu + \lambda} \text{tr}^2(G) + 2\mu|G|^2, \quad Q_D^2(G) := 4c|G|^2, \quad c > 0$$

for every symmetric $G \in \mathbb{R}_{\text{sym}}^{2 \times 2}$. The constants λ, μ are the Lamé constants from (5.3) and $c > 0$ is the same viscosity parameter as in (5.1).

We then compare the solution of the thin-plate model with a full three-dimensional simulation using the algorithm from the beginning of Section 5 developed in this article, applied to a 3d plate with thickness h in a reference domain $\omega \times (-\frac{1}{2}, \frac{1}{2})$ and x_3 derivative rescaled by $\frac{1}{h}$. The initial configuration is given as the respective element of the recovery sequence for v, u above, as detailed in [10, Section 6.2], yielding approximately the same starting energy as the thin-plate limit. The simulation was performed using 201,514 tetrahedra resulting in 818,538 degrees of freedom. The wall time to full relaxation at $t \approx 30$ was approximately 6 days on 8 cores of an Intel Xeon Gold 6230.

The parameters of this experiment are $\mu = \lambda = 1.0 \cdot 10^3$, $c = 3.0 \cdot 10^3$ and $h = 0.1$. The time-step size for the plate simulation was $\tau_{\text{plate}} = 1$, for the 3d simulation it was $\tau_{3d} = 0.01$. A comparison of midplane deformation in the 3d simulation with the limiting plate model is shown in Figure 1. Figure 2 shows the 3d deformation at a $t = 2$, as well as a comparison of the energy and cumulative dissipation of the plate model and the 3d simulation (see also the convergence study below). One can clearly see that our model and the plate limit yield very similar results, as one would expect. We also point out the near perfect adherence to energy-dissipation equality by the 3d simulations using the method developed here.

Experiment 2: Jello. We simulate the viscous evolution of a rectangular block of a material attached at the top under the influence of a gravitational body force. The jello has a reference configuration that occupies a domain $\Omega = (-1, 1) \times (-1, 1) \times (-\frac{1}{2}, \frac{1}{2})$ and an initial condition $y(x) = x$. A Dirichlet boundary condition fixes $y|_{\{x_3=\frac{1}{2}\}} = x$ for all time. The energy is a sum of the Neo-Hookean energy in (5.3) and $-\int_{\Omega} f y_3 \, dx$. The parameters in this simulation are $\mu = 1.0 \cdot 10^3$, $\lambda = 1.5 \cdot 10^3$, $f = -2.0 \cdot 10^3$, $c = 3.0 \cdot 10^3$, and $\tau = 0.01$. Again, we see nearly perfect adherence to the energy-dissipation balance in this simulation. The number of degrees of freedom and the running time are the same as for Experiment 1 above. The results are illustrated in Figure 3.

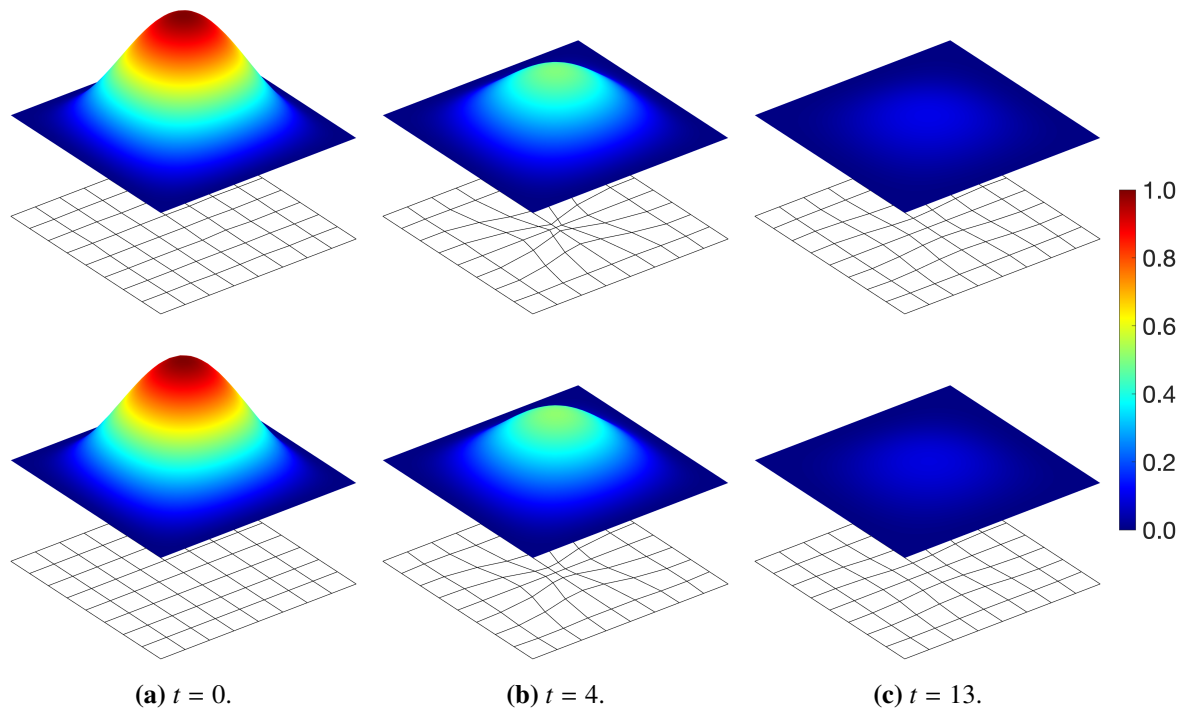
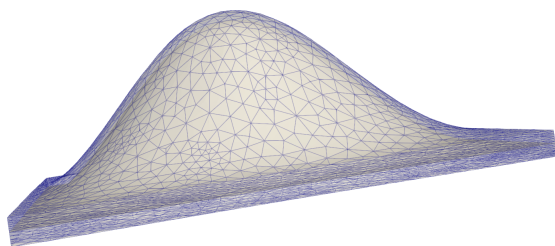
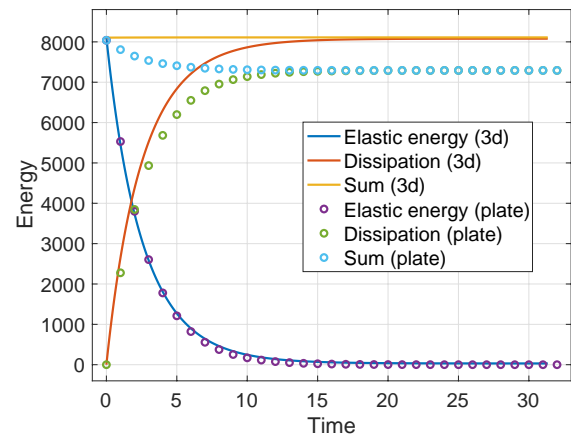


Figure 1. Comparison of the simulation results using the 3d visco-elasticity method introduced here (top row, shown are out-of-plane (v) and in-plane (u) deformation of the mid-plane of the 3d plate) and the results using the limiting viscoelastic Föppl-von Kármán plate using the method of [9] (bottom row). The in-plane deformation is exaggerated by a factor of 6.



(a) A 3d deformation at $t = 2$. The mid-plane (which is also seen in Figure 1) is plotted opaque, the remaining material is transparent. The surface triangles of the tetrahedral mesh are shown in blue. The out-of-plane deformation has been rescaled according to the Föppl-von Kármán scaling.



(b) The potential energy, the cumulative dissipation and their sum. The results from the 2d plate simulation are shown as circles; the solid lines correspond to the 3d simulation.

Figure 2. The 3d-deformation state and the time-dependent elastic and dissipated energy.

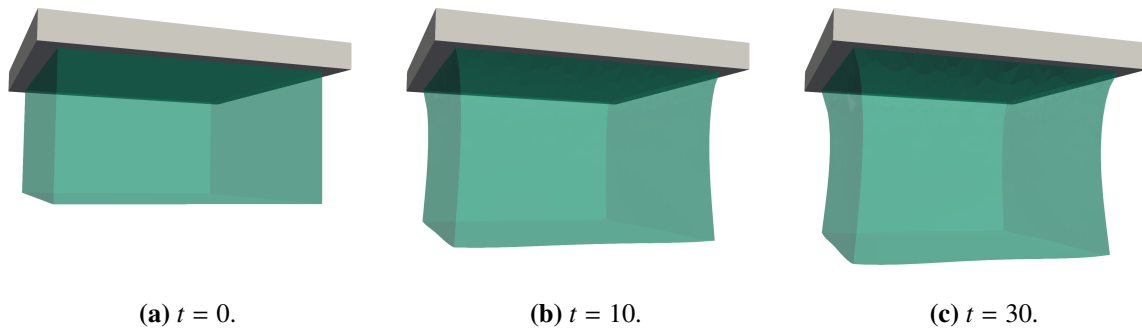


Figure 3. Simulation results for the visco-elastic (jello) material. The plate at the top indicates where the specimen is fixed; a gravitational body force acts downwards.

Convergence study. We performed a simple study testing the relative error in the energy-dissipation equality according to the time-step size τ . In the reference domain $\Omega = (-1, 1)^3$, we choose an initial condition

$$y^0 = \begin{pmatrix} 1.2 & 0 & 0 \\ 0 & 1 & 0 \\ 0 & 0 & 1 \end{pmatrix} x$$

and perform the *linearized* time-stepping scheme in (5.2) until final time $T = 1$, i.e., up to step $K_\tau = \frac{1}{\tau}$ for time steps $\tau \in \{0.1, 0.01, 0.001\}$. Finally, we compute the relative error in the energy-dissipation equality with the *nonlinear* dissipation distance, i.e., we compute

$$e_\tau = \frac{\left| W(y^0) - W(y^{K_\tau}) - \sum_{j=1}^{K_\tau} D(\nabla y^j, \nabla y^{j-1}) \right|}{\sum_{j=1}^{K_\tau} D(\nabla y^j, \nabla y^{j-1})}.$$

The simulation was performed using the parameters $\mu = 1.0 \cdot 10^3$, $\lambda = 1.5 \cdot 10^3$, $c = 3.0 \cdot 10^3$, no body force and stress-free boundary conditions on a domain discretized using 147 342 P2 finite elements. From Figure 4 one can clearly obtain that $e_\tau = \mathcal{O}(\tau)$. The same scaling is also obtained using coarser discretizations with 71,369 and 33,216 P2 finite elements. We thus conclude that our linearized time-stepping scheme recovers the correct energy-dissipation equality for nonlinear Kelvin-Voigt visco-elasticity.

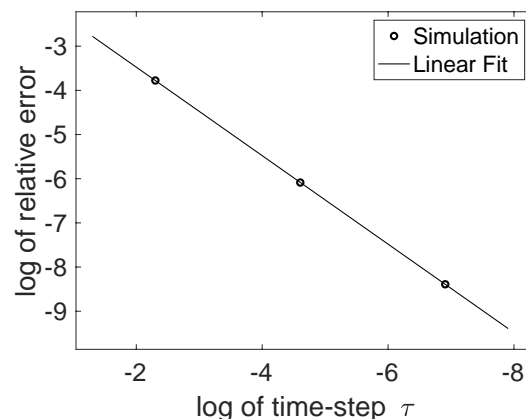


Figure 4. Simulation using 147,342 P2 finite elements. The slope of the linear fit is 1.00.

Acknowledgements

PD and MJ are grateful for the hospitality afforded by The Institute of Information Theory and Automation of the Czech Academy of Sciences. MJ and MK acknowledge the support from the University of Freiburg during their stays there. PD acknowledges support by the state of Baden-Württemberg through bwHPC and from the DFG via project 441523275 in SPP 2256. MK and JV were supported by the GAČR project 21-06569K and by the MŠMT ČR project 8J21AT001 Model Reduction and Optimal Control in Thermomechanics. MK also thanks the ESI Vienna for its hospitality during his stay in January-February 2022.

Conflict of interest

The authors declare no conflict of interest.

References

1. S. S. Antman, Physically unacceptable viscous stresses, *Z. Angew. Math. Phys.*, **49** (1998), 980–988. <https://doi.org/10.1007/s000330050134>
2. S. S. Antman, *Nonlinear problems of elasticity*, 2 Eds., New York: Springer, 2005. <https://doi.org/10.1007/0-387-27649-1>
3. J. M. Ball, Y. Şengül, Quasistatic nonlinear viscoelasticity and gradient flows, *J. Dyn. Diff. Equat.*, **27** (2015), 405–442. <https://doi.org/10.1007/s10884-014-9410-1>
4. F. K. Bogner, R. L. Fox, L. A. Schmit, The generation of interelement compatible stiffness and mass matrices by the use of interpolation formulas, In: *Proc. Conf. Matrix Methods in Struct. Mech*, AirForce Inst. of Tech, Wright Patterson AF Base, Ohio, 1965, 397–444.
5. Y. Chen, T. A. Davis, W. W. Hager, S. Rajamanickam, Algorithm 887: CHOLMOD, Supernodal sparse Cholesky factorization and update/downdate, *ACM Trans. Math. Software*, **35** (2008), 22. <https://doi.org/10.1145/1391989.1391995>
6. B. Dacorogna, *Direct methods in the calculus of variations*, 2 Eds., New York: Springer, 2008. <https://doi.org/10.1007/978-0-387-55249-1>
7. G. Dal Maso, M. Negri, D. Percivale, Linearized elasticity as Γ -limit of finite elasticity, *Set-Valued Analysis*, **10** (2002), 165–183. <https://doi.org/10.1023/A:1016577431636>
8. M. Friedrich, M. Kružík, On the passage from nonlinear to linearized viscoelasticity, *SIAM J. Math. Anal.*, **50** (2018), 4426–4456. <https://doi.org/10.1137/17M1131428>
9. M. Friedrich, M. Kružík, J. Valdman, Numerical approximation of von Kármán viscoelastic plates, *Discrete Cont. Dyn. Syst. S*, **14** (2021), 299–319. <https://doi.org/10.3934/dcdss.2020322>
10. G. Friesecke, R. D. James, S. Müller, A hierarchy of plate models derived from nonlinear elasticity by Gamma-convergence, *Arch. Rational Mech. Anal.*, **180** (2006), 183–236. <https://doi.org/10.1007/s00205-005-0400-7>
11. S. Krömer, T. Roubíček, Quasistatic viscoelasticity with self-contact at large strains, *J. Elast.*, **142** (2020), 433–445. <https://doi.org/10.1007/s10659-020-09801-9>

12. A. Mielke, C. Ortner, Y. Şengül, An approach to nonlinear viscoelasticity via metric gradient flows, *SIAM J. Math. Anal.*, **46** (2014), 1317–1347. <https://doi.org/10.1137/130927632>
13. P. Neff, On Korn's first inequality with non-constant coefficients, *Proc. Roy. Soc. Edinb. A*, **132** (2002), 221–243. <https://doi.org/10.1017/S0308210500001591>
14. J. Valdman, MATLAB implementation of C1 finite elements: Bogner-Fox-Schmit rectangle, In: *Parallel processing and applied mathematics. PPAM 2019*, Cham: Springer, 2020, 256–266. https://doi.org/10.1007/978-3-030-43222-5_22



AIMS Press

© 2023 the Author(s), licensee AIMS Press. This is an open access article distributed under the terms of the Creative Commons Attribution License (<http://creativecommons.org/licenses/by/4.0>)